Weierstraß-Institut
für Angewandte Analysis und Stochastik

im Forschungsverbund Berlin e.V.

Preprint ISSN 0946 – 8633

Monochromatic Surface Waves at the Interface between Poroelastic and Fluid Halfspaces

Bettina Albers

submitted: 21st February 2005

Weierstrass Institute
for Applied Analysis
and Stochastics
Mohrenstrasse 39
10117 Berlin
Germany
E-Mail: albers@wias-berlin.de

No. 1010
Berlin 2005

2000 *Mathematics Subject Classification.* 74J15, 76S05, 74S99.

Key words and phrases. Surface waves, flows in porous media, numerical analysis of dispersion relation.

Dedicated to my friend and teacher Prof. Krzysztof Wilmanski on the occasion of his 65th anniversary.

Edited by
Weierstraß-Institut für Angewandte Analysis und Stochastik (WIAS)
Mohrenstraße 39
10117 Berlin
Germany

Fax: + 49 30 2044975
E-Mail: preprint@wias-berlin.de
World Wide Web: http://www.wias-berlin.de/

a

Abstract

The topic of the previous work [4] was the study of monochromatic surface waves at the boundary between a porous medium and a vacuum. This article is an extension of this research to the propagation of surface waves on the interface between a porous halfspace and a fluid halfspace. Results for phase and group velocities and attenuations are shown in dependence on both the frequency and the surface permeability. In contrast to classical papers on surface waves (e.g. [12]) where only the limits of the frequency $\omega \to 0$, $\omega \to \infty$ and the limits of the surface permeability (fully sealed and fully open boundary) were studied, we investigate the problem in the full range of both parameters.

For the analysis we use the "simple mixture model" which is a simplification of the classical Biot model for poroelastic media. The construction of a solution is shown and the dispersion relation solved numerically.

There exist three surface waves for this boundary: a leaky Rayleigh wave and both a true and a leaky Stoneley wave. The true Stoneley wave exists only in a limited range of the surface permeability.

1 Introduction

This paper is a continuation of the work [4] on the numerical analysis of surface waves in poroelastic media. In the previous paper the frequency dependence of monochromatic surface waves at the boundary of a poroelastic halfspace and vacuum was shown. Whereas at a plane boundary of a homogeneous linear elastic material solely a true Rayleigh wave appears, at the boundary of the porous medium with vacuum this wave becomes leaky and additionally a second surface wave, a true Stoneley wave, emerges. This is the consequence of the principle of constructive interference [17].

A true surface wave propagates along the direction parallel to the surface and decays exponentially with depth, while leaky surface waves are attenuated in the surface direction and radiate energy into bulk or other surface waves. It is customary in the literature on waves in porous materials to call leaky surface waves pseudosurface waves (e.g. [12], [8],

[a] Dedicated to my friend and teacher Prof. Krzysztof Wilmanski on the occasion of his 65th anniversary.

first used in [14]), i.e. a *leaky surface wave is identical with a pseudosurface wave*. In this article we prefer to call these waves *leaky surface waves* (as e.g. done in [16]).

In the present article the boundary a porous medium and an ideal fluid is investigated. This means that we have one additional component compared to the boundary porous medium/vacuum. Thus, besides the three bulk waves in the porous medium (fast longitudinal wave $P1$, slow longitudinal wave $P2$ and transversal wave S) there exists also a P-wave in the fluid. These four waves combine into three surface waves: a leaky Rayleigh wave and both a true and a leaky Stoneley wave. Their acoustic properties (phase and group velocities, attenuations) will be shown in this paper in dependence on two quantities: the frequency ω and the surface permeability parameter α.

In contrast to earlier works in this field, we investigate the acoustic properties of surface waves in the whole range of both parameters. Only in the work of Gubaidullin et al. [13] these properties were analyzed for all frequencies but only for the two limit values of the surface permeability α ($\frac{1}{T}$ in their notation). In spite of the use of the full Biot model and another analytical method of investigation results presented in the work [13] coincide with our results for the two limit values of α.

The investigation of the full range of frequencies reveals that the transition from low frequencies to high frequencies is not monotonous or even smooth. As intermediate frequencies are essential for practical purposes such an investigation becomes paramount importance. Practical ranges may vary from 100 MHz in electronic industry (e.g. the testing of surface coatings by nanomaterials) to 1 to 100 Hz for field testing of soils and rocks in geophysics. Intermediate frequencies appear as well, e.g. in civil engineering and medicine.

Non-invasive testing methods in all those fields are primarily based on an analysis of surface waves. The recently developed method of nondestructive testing of soils, SASW (Spectral Analysis of Surface Waves) (see e.g. [15]) which is based on the theory of classical Rayleigh waves in inhomogeneous materials shows how useful such theoretical results are.

Apart from the frequency range, also properties of the boundary described by the surface permeability are investigated in the present work. The variation of this second parameter, α, which controls the intensity of the in- and outflow of the fluid from the porous medium, brought to light that the true Stoneley wave exists only for very small values of this parameter, i.e. for a boundary which is almost sealed. Attenuations of both leaky waves show an interesting behavior in dependence on the frequency: for two frequencies there appear resonance effects. They seem to be not only theoretically but also experimentally observed [8] and may be related to characteristic frequencies of the solid and the fluid, respectively.

2 Theoretical background

2.1 Biot's model

The most popular and widespread model for the theoretical description of linear processes in fluid-saturated poroelastic media is the *Biot model* [7]. It is based on the following

momentum balances

$$\rho_0^F \frac{\partial \mathbf{v}^F}{\partial t} = \kappa \rho_0^F \operatorname{grad} \varepsilon + Q \operatorname{grad} \operatorname{tr} \mathbf{e}^S - \pi \left(\mathbf{v}^F - \mathbf{v}^S \right) + \rho_{12} \left(\frac{\partial \mathbf{v}^F}{\partial t} - \frac{\partial \mathbf{v}^S}{\partial t} \right), \tag{1}$$

$$\rho_0^S \frac{\partial \mathbf{v}^S}{\partial t} = \lambda^S \operatorname{grad} \operatorname{tr} \mathbf{e}^S + 2\mu^S \operatorname{div} \mathbf{e}^S + Q \operatorname{grad} \varepsilon + \pi \left(\mathbf{v}^F - \mathbf{v}^S \right) - \rho_{12} \left(\frac{\partial \mathbf{v}^F}{\partial t} - \frac{\partial \mathbf{v}^S}{\partial t} \right),$$

where $\mathbf{v}^F, \mathbf{v}^S$ are the macroscopic (average) partial velocities of the fluid and of the skeleton, respectively, $\mathbf{e}^S$ denotes the symmetric Almansi-Hamel tensor of small deformations of the skeleton, ε is the volume change of the fluid. They fulfil the following relations

$$\frac{\partial \mathbf{e}^S}{\partial t} = \operatorname{sym} \operatorname{grad} \mathbf{v}^S, \quad \frac{\partial \varepsilon}{\partial t} = \operatorname{div} \mathbf{v}^F,$$
$$\varepsilon := \frac{\rho_0^F - \rho^F}{\rho_0^F}, \quad \zeta := n_0 (\operatorname{tr} \mathbf{e}^S - \varepsilon); \tag{2}$$

where ζ denotes the change of fluid contents commonly used as a field in Biot's model instead of ε. If we introduce partial displacement fields $\mathbf{u}^S \equiv \mathbf{u}$, $\mathbf{u}^F \equiv \mathbf{U}$, then

$$\mathbf{e}^S = \operatorname{sym} \operatorname{grad} \mathbf{u}, \quad \mathbf{v}^S = \frac{\partial \mathbf{u}}{\partial t}, \quad \varepsilon = \operatorname{div} \mathbf{U}, \quad \mathbf{v}^F = \frac{\partial \mathbf{U}}{\partial t}. \tag{3}$$

The quantities $\rho_0^F = n_0 \rho_0^{FR}$, $\rho_0^S = (1 - n_0)\, \rho_0^{SR}$ denote constant (initial) mass densities, ρ_0^{FR}, ρ_0^{SR} are the initial true mass densities, n_0 is the initial porosity. The material parameters $\lambda^S, \mu^S, \kappa, Q, \pi, \rho_{12}$ are assumed to be constant. The parameter Q describes the coupling of partial stresses in the Biot's model, while ρ_{12} is attributed to the tortuosity a. The permeability coefficient π corresponds to the classical Darcy coefficient.

The problem of the frequency dependence for intermediate frequencies has for a long time been ignored in the literature, mostly due to numerical difficulties within Biot's model.

One of the first attempts, e.g., to investigate surface waves in two-component porous materials stems from Deresiewicz [9]. In this paper he has studied the boundary porous medium/vacuum using the Biot equations. He has numerically calculated Rayleigh wave velocities and attenuations. But he wrote: "*Because of its complexity, the secular* (i.e. dispersion; B.A.) *equation does not lend itself to analytical study for intermediate values of the frequency. Accordingly, a numerical study was undertaken, of the variation of velocity and dissipation per cycle with frequency, for a material whose elastic and dynamical coefficients were available, with several curious results.*" One of these "curious" results is a minimum of the phase velocity in the region of small frequencies which we also found for the Rayleigh wave [4]. It is impressing how much the author did know about the Rayleigh wave already in the 60ies. However, it is strange that he did not get the Stoneley solution from the dispersion equation.

Feng & Johnson [12] use Biot's theory to search numerically primarily the velocities of various surface waves. They distinguish between the true slow surface wave and the leaky surface waves and calculate their velocities at an interface between a fluid half-space and a half space of a fluid-saturated porous medium as we do as well in the sequel. However, they rely on a somewhat different approach to obtain results for the surface waves. In contrast to our approach, Feng & Johnson focus only on the high-frequency range and they limit

their attention to the open-pore and to the sealed pore situation (i.e. in our notation: $\alpha = \infty$ and $\alpha = 0$, respectively, and in their notation: $T = 0$ and $T = \infty$). In dependence on the stiffness of the skeleton (in their notation: longitudinal modulus of the skeleton frame $\left(K_b + \frac{4}{3}N\right)^{1/2}$, where K_b : bulk modulus of porous drained solid, N : shear modulus of the drained porous solid) and e.g. on the coefficient of added mass ("tortuosity", in their notation: α) they have investigated the existence of the surface modes. Their numerical results for material parameters for water as the fluid (in both $z < 0$ and $z > 0$ regions) and fused glass beads as the porous medium agree with our results. Otherwise the ranges of investigation of Feng & Johnson and ours do not coincide. In order to compare the results we have calculated the stiffness of the sandstone of our example in their notation. For the first set of parameters $\left(K_b + \frac{4}{3}N\right)^{1/2} \approx 3.95 \cdot 10^5 \frac{\sqrt{\text{dynes}}}{\text{cm}}$, for the other one $5.53 \cdot 10^5 \frac{\sqrt{\text{dynes}}}{\text{cm}}$. Feng & Johnson investigate a range $0 \leq \sqrt{K_b + \frac{4}{3}N} \leq 7 \cdot 10^5 \frac{\sqrt{\text{dynes}}}{\text{cm}}$. They found that for an open-pore surface situation, the true surface wave exists for a limited range of material parameters and changes continuously into a slightly leaky Stoneley wave as its velocity crosses over the slowest bulk wave velocity. For the sealed pore situation there exist simultaneously a true surface wave (for all values of material parameters) and a leaky Stoneley wave.

2.2 Simple mixture model

In our analysis we rely on a simpler model than this of Biot. We neglect two effects:

- the added mass effect reflected in Biot's model by off-diagonal contributions to the matrix of partial mass densities (the parameter ρ_{12}),
- the static coupling effect between partial stresses (the parameter Q).

The first one is neglected because it yields a non-objectivity of Biot's equations and, additionally, an unphysical dependence of the attenuation on the tortuosity (see: [22], [20]).

The second contribution, the coupling of partial stresses Q, is neglected because it yields only *quantitative* corrections without changing the *qualitative* behavior of the system, at least in the range of a relatively high stiffness of the skeleton in comparison with the fluid. This has been analyzed for bulk waves in [3].

Bearing these remarks in mind it seems to be appropriate to rely on the simplified model ("simple mixture model" in which $Q = 0$, $\rho_{12} = 0$). It has the advantage to reduce essentially technical difficulties.

We present here the linear form of the "simple mixture" model for a two-component poroelastic saturated medium (for details see: [23]).

As it is done in the Biot model, in the simple mixture model, a process is described by the *macroscopic* fields $\rho^F(\mathbf{x},t)$, the partial mass density of the fluid, $\mathbf{v}^F(\mathbf{x},t)$, $\mathbf{v}^S(\mathbf{x},t)$, the velocities of the fluid and of the skeleton, respectively, $\mathbf{e}^S(\mathbf{x},t)$, the symmetric tensor of small deformations of the skeleton and n, the porosity. The following set of linear equations is satisfied by those fields

$$\frac{\partial \rho^F}{\partial t} + \rho_0^F \operatorname{div} \mathbf{v}^F = 0, \quad \left|\frac{\rho^F - \rho_0^F}{\rho_0^F}\right| \ll 1, \tag{4}$$

$$
\begin{aligned}
&\rho_0^F \frac{\partial \mathbf{v}^F}{\partial t} + \kappa \operatorname{grad} \rho^F + \beta \operatorname{grad}(n - n_E) + \hat{\mathbf{p}} = 0, \quad \hat{\mathbf{p}} := \pi\left(\mathbf{v}^F - \mathbf{v}^S\right), \\
&\rho_0^S \frac{\partial \mathbf{v}^S}{\partial t} - \operatorname{div}\left(\lambda^S \left(\operatorname{tr} \mathbf{e}^S\right) \mathbf{1} + 2\mu \mathbf{e}^S + \beta (n - n_E)\, \mathbf{1}\right) - \hat{\mathbf{p}} = 0, \qquad (4)_{\text{cont.}} \\
&\frac{\partial \mathbf{e}^S}{\partial t} = \operatorname{sym} \operatorname{grad} \mathbf{v}^S, \quad \left\|\mathbf{e}^S\right\| \ll 1, \quad n_E := n_0\left(1 + \delta \operatorname{tr} \mathbf{e}^S\right), \\
&\frac{\partial (n - n_E)}{\partial t} + \Phi \operatorname{div}\left(\mathbf{v}^F - \mathbf{v}^S\right) + \frac{n - n_E}{\tau_n} = 0, \quad \left|\tfrac{n - n_0}{n_0}\right| \ll 1.
\end{aligned}
$$

We have already introduced ρ_0^F, ρ_0^S, n_0, which are the constant reference values of partial mass densities, and porosity, respectively. There appear also constant material parameters $\kappa, \lambda^S, \mu^S, \beta, \pi, \tau_n, \delta, \Phi$. In particular, κ denotes the macroscopic compressibility of the fluid component, λ^S and μ^S are macroscopic elastic constants of the skeleton, β is the coupling constant between the components, π denotes the bulk permeability coefficient, τ_n describes the relaxation time of porosity and δ, Φ are equilibrium and nonequilibrium changes of porosity, respectively. As we have already done in the work [4] for the analysis of surface waves the coupling parameter β is assumed to be zero. Then the problem of evolution of porosity described by equation $(4)_5$ can be solved separately from the rest of the problem. We investigate the approximation of a very large relaxation time of porosity ($\tau_n \to \infty$) compared to the inverse of characteristic frequencies. This is justified in applications to soils where viscous effects related to porosity do not seem to appear. Then the nonequilibrium porosity n is determined by volume changes of the skeleton and of the fluid: $n = n_E + \Phi\left(\operatorname{tr} \mathbf{e}^S - \varepsilon\right)$. Consequently, they do not give any independent contribution to the wave problem.

2.3 Boundary conditions

For the determination of surface waves in saturated poroelastic media conditions for $z = 0$ are needed. We are going to consider the interface between a saturated porous material and an ideal fluid. Boundary conditions for such an interface were formulated by Deresiewicz & Skalak [10]. Here we have slightly changed their notation. The quantities outside of the porous medium are denoted by a sub- or superscript "+" sign. Then the boundary conditions have the following form

- $\left(T_{13} - T_{13}^+\right)\big|_{z=0} \equiv T_{13}^S\big|_{z=0} = c_S^2 \rho_0^S \left(\dfrac{\partial u_1^S}{\partial z} + \dfrac{\partial u_3^S}{\partial x}\right)\Big|_{z=0} = 0,$
- $\left(T_{33} - T_{33}^+\right)\big|_{z=0} \equiv \left(T_{33}^S + p^{F+} - p^F\right)\big|_{z=0} =$
$$
\begin{aligned}
&= c_{P1}^2 \rho_0^S \left(\frac{\partial u_1^S}{\partial x} + \frac{\partial u_3^S}{\partial z}\right) - 2c_S^2 \rho_0^S \frac{\partial u_1^S}{\partial x} + \\
&\quad + c_+^2 \left(\rho^{F+} - \rho_0^{F+}\right) - c_{P2}^2 \left(\rho^F - \rho_0^F\right)\big|_{z=0} = 0, \qquad (5)
\end{aligned}
$$
- $\rho_0^F \dfrac{\partial}{\partial t}\left(u_3^F - u_3^S\right)\Big|_{z=0} = \rho_0^{F+} \dfrac{\partial}{\partial t}\left(u_3^{F+} - u_3^S\right)\Big|_{z=0},$
- $\rho_0^F \dfrac{\partial}{\partial t}\left(u_3^F - u_3^S\right) + \alpha\left(p^F - n_0 p^{F+}\right)\Big|_{z=0} = 0.$

Here u_1^S, u_3^S are x-, and z-components of the displacement $\mathbf{u}^S$, respectively, and u_3^F, u_3^{F+} denote z-components of the displacements $\mathbf{u}^F$ and $\mathbf{u}^{F+}$, respectively. Simultaneously,

$$c_{P1}^2 := \frac{\lambda^S + 2\mu^S}{\rho_0^S}, \quad c_S^2 := \frac{\mu^S}{\rho_0^S}, \quad c_{P2}^2 := \kappa, \quad c_+^2 := \kappa^+, \tag{6}$$

are squares of the front velocities of the bulk waves in the porous material: $P1$ (fast wave), S (shear wave), $P2$ (slow wave, also called Biot's wave), and of the P-wave in the fluid, respectively. In the case of Biot's model there would be an additive contribution in the numerator of c_{P1} of the coupling parameter Q which is of the order of a few percent of λ^S (see: Albers, Wilmanski [3] for a detailed analysis).

Two of the boundary conditions, $(5)_1$ and $(5)_2$, describe the continuity of the full traction, $\mathbf{t} := \left(\mathbf{T}^S + \mathbf{T}^F\right)\mathbf{n}$, $\mathbf{n} = (0,0,1)^T$, on the boundary; $(5)_3$ reflects the continuity of the fluid mass flux, and condition $(5)_4$ specifies the mass transport through the surface. The difference of the pore pressures on both sides of the boundary determines the in- and outflow through the boundary. α denotes a surface permeability coefficient, which corresponds to $\frac{1}{T}$ in the works [12], [13], and p^{F+} is the external pressure. Condition $(5)_4$ relies on the assumption that the pore pressure p and the partial pressure p^F satisfy the relation $p^F \approx n_0 p$ at least in a small vicinity of the surface.

Some words are appropriate to explain the notion of *surface permeability*: Figure 1 demonstrates a Gedankenexperiment which explains the origin of surface effects. The flow of the fluid is "straight" both outside the porous medium and inside the channels of the porous medium. However, at the entrance to the porous medium the flow is disturbed: the fluid has to find its way through the voids between the solid particles. In principle we consider a flow which is perpendicular to the boundary but in a small boundary layer it deviates from this direction. A detailed structure of the boundary determines the resistance against the inflow and, consequently, the surface permeability α. The value $\alpha = 0$ corresponds to a sealed pore situation, for $\alpha = \infty$ the boundary is completely open.

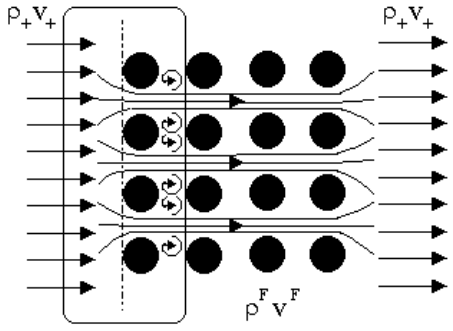

Fig. 1: Sketch of the flow into and out of a porous medium.

3 Construction of the solution

3.1 Introduction

Investigating the interface between a porous medium and a liquid we have to consider additional equations for the liquid outside of the porous medium. We distinguish this part of the system by the sign "+".

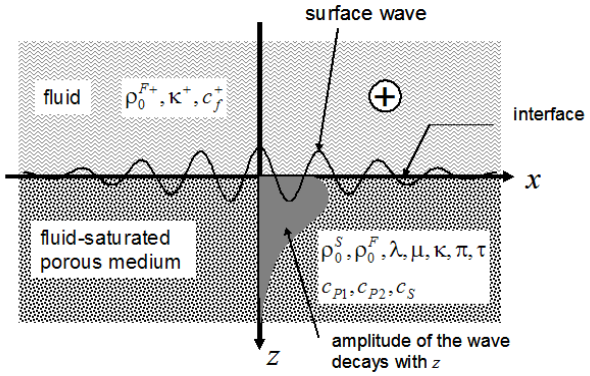

Fig. 2: Geometry of the interface porous medium/fluid.

The procedure of the construction of the solutions which is used in this work has already been applied in earlier works (see e.g. [21], [11], [24] or [4]). While in [11] an asymptotic analysis of the high-frequency properties of surface waves in function of the wavelength $1/k$ (k – wave number) within the simple mixture model was carried out, here and in the other papers, we consider monochromatic waves with a given *real frequency* ω. This is necessary for the investigation of a far field boundary value problem with a harmonic surface source of waves.

The additional equations for the fluid in the exterior of the porous material read

$$\frac{\partial \rho^{F+}}{\partial t} + \rho_0^{F+} \operatorname{div} \mathbf{v}^{F+} = 0, \qquad \rho_0^{F+} \frac{\partial \mathbf{v}^{F+}}{\partial t} + \kappa^+ \operatorname{grad} \rho^{F+} = 0. \tag{7}$$

Here ρ^{F+} denotes the partial mass density of the fluid in the +-region and ρ_0^{F+} is its constant reference value. κ^+ describes the compressibility of the fluid.

> **Comment:** The identification of compressibility coefficients in porous materials can be done in many ways and they do not necessarily give the same results. To make this issue clear, we present here two approaches.
>
> One of them is commonly used in micro-macro transitions for granular materials. Such a transition is described by relations $\rho^F = n\rho^{F+}$, $p^F = np^{F+}$, $p^F - p_0^F = \kappa\left(\rho^F - \rho_0^F\right)$, $p^{F+} - p_0^{F+} = \kappa^+\left(\rho^{F+} - \rho_0^{F+}\right)$, and, under the condition of constant porosity $n = n_0$, we have $\kappa = \kappa^+$.
>
> However, a simple wave analysis shows that this relation cannot hold for dynamical processes as the speeds of waves carried by the fluid component are, respectively, $c_+ = \sqrt{\kappa^+}$, $c_{P2} = \sqrt{\kappa}$, and these are, of course, different. The situation does not improve essentially if we introduce Biot's coupling. This means that linear models used in the description of waves cannot be based on the above quoted simple micro-macro relations. They possess their own macroscopic status and their effective material parameters account for such microscopic effects as scattering of waves. Different macroscopic compressibilities for the same material inside and outside of the porous medium are caused by the channels of the porous medium. While a wave can take a free "path" in the fluid outside, inside the porous medium waves are slower due to reflection on the boundaries of the channels. This is, certainly, not present in simple micro-macro transitions.
>
> We assume the fluid to be water. A wave in water travels with the velocity of around $c_+ \approx 1500\ \frac{\mathrm{m}}{\mathrm{s}}$ and the corresponding compressibility $\kappa^+ = 2.25 \cdot 10^6\ \frac{\mathrm{m}^2}{\mathrm{s}^2}$. Inside the porous medium the velocity of the $P2$-wave is assumed to be $c_{P2} = 1000\ \frac{\mathrm{m}}{\mathrm{s}}$ to which corresponds a compressibility $\kappa = c_{P2}^2 = 1 \cdot 10^6\ \frac{\mathrm{m}^2}{\mathrm{s}^2}$.

3.2 Compatibility with field equations

We introduce the displacement vectors $\mathbf{u}^S$, $\mathbf{u}^F$ and $\mathbf{u}^{F+}$ for the skeleton, for the fluid inside the porous medium and for the fluid outside the porous medium, respectively. Both latter quantities do not have any direct physical bearing. They are introduced only for the technical symmetry of considerations. According to Helmholtz's Theorem we have then

$$\begin{aligned}
&\mathbf{u}^S = \operatorname{grad}\varphi^S + \operatorname{rot}\boldsymbol{\psi}^S, \quad \mathbf{v}^S = \frac{\partial \mathbf{u}^S}{\partial t}, \quad \mathbf{e}^S = \operatorname{sym}\operatorname{grad}\mathbf{u}^S, \\
&\mathbf{u}^F = \operatorname{grad}\varphi^F + \operatorname{rot}\boldsymbol{\psi}^F, \quad \mathbf{v}^F = \frac{\partial \mathbf{u}^F}{\partial t}, \\
&\mathbf{u}^{F+} = \operatorname{grad}\varphi^{F+}, \quad \mathbf{v}^{F+} = \frac{\partial \mathbf{u}^{F+}}{\partial t}.
\end{aligned} \tag{8}$$

The following solutions for monochromatic waves in the x-direction are considered for the two-dimensional case

$$\begin{aligned}
\varphi^S &= A^S(z)\exp\left[i\left(kx-\omega t\right)\right], \quad \varphi^F = A^F(z)\exp\left[i\left(kx-\omega t\right)\right], \\
\psi_y^S &= B^S(z)\exp\left[i\left(kx-\omega t\right)\right], \quad \psi_y^F = B^F(z)\exp\left[i\left(kx-\omega t\right)\right], \\
\varphi^{F+} &= A^{F+}(z)\exp\left[i\left(kx-\omega t\right)\right], \quad \psi_x^S = \psi_z^S = \psi_x^F = \psi_z^F = 0, \\
\rho^F - \rho_0^F &= A_\rho^F(z)\exp\left[i\left(kx-\omega t\right)\right], \quad \rho^{F+} - \rho_0^{F+} = A_\rho^{F+}(z)\exp\left[i\left(kx-\omega t\right)\right].
\end{aligned} \tag{9}$$

They are substituted in the field equations of the simple mixture model ((4) without balance of porosity and (7)). This leads to the following compatibility conditions

$$\begin{aligned}
&B^F = \frac{i\pi}{\rho_0^F\omega + i\pi}B^S, \qquad A_\rho^F = -\rho_0^F\left(\frac{d^2}{dz^2}-k^2\right)A^F, \\
&\left[\kappa\left(\frac{d^2}{dz^2}-k^2\right)+\omega^2\right]A^F + \frac{i\pi}{\rho_0^F}\omega\left(A^F - A^S\right) = 0, \\
&\left[\frac{\lambda^S+2\mu^S}{\rho_0^S}\left(\frac{d^2}{dz^2}-k^2\right)+\omega^2\right]A^S - \frac{i\pi}{\rho_0^S}\omega\left(A^F - A^S\right) = 0, \\
&\left[\frac{\mu^S}{\rho_0^S}\left(\frac{d^2}{dz^2}-k^2\right)+\omega^2 + \frac{i\pi\rho_0^F}{\rho_0^S\left(\rho_0^F\omega + i\pi\right)}\omega^2\right]B^S = 0,
\end{aligned} \tag{10}$$

as well as

$$A_\rho^{F+} = -\rho_0^{F+}\left(\frac{d^2}{dz^2}-k^2\right)A^{F+}, \qquad \left[\kappa^+\left(\frac{d^2}{dz^2}-k^2\right)+\omega^2\right]A^{F+} = 0. \tag{11}$$

3.3 Dimensionless notation

A dimensionless notation has the advantage to connect characteristics of the surface waves to those of the better known bulk waves (e.g. with the velocity of the $P1$-wave c_{P1}). To

this aim some dimensionless quantities are defined

$$
\begin{aligned}
c_s &:= \frac{c_S}{c_{P1}} < 1, \quad c_f := \frac{c_{P2}}{c_{P1}}, \quad \pi' := \frac{\pi\tau}{\rho_0^S} > 0, \\
r &:= \frac{\rho_0^F}{\rho_0^S} < 1, \qquad z' := \frac{z}{c_{P1}\tau}, \quad k' := kc_{P1}\tau, \quad \omega' := \omega\tau, \\
c_f^+ &:= \frac{\sqrt{\kappa^+}}{c_{P1}}, \quad r^+ := \frac{\rho_0^{F+}}{\rho_0^S} < 1, \quad \alpha' := \alpha c_{P1}.
\end{aligned}
\tag{12}
$$

Here τ is an arbitrary reference time. It may be chosen as $\tau = \frac{\rho_0^S}{\pi}$ which would lead to $\pi' = 1$, or it may be identical with the relaxation time of porosity τ_n. Further, we make an arbitrary choice of this normalization parameter.

3.4 Ansatz

For simplicity we further omit the prime in (12). Substitution of these quantities in equations (10) and (11) yields

$$
\begin{aligned}
\left[c_f^2\left(\frac{d^2}{dz^2} - k^2\right) + \omega^2\right] A^F + i\frac{\pi}{r}\omega\left(A^F - A^S\right) &= 0, \\
\left[\left(\frac{d^2}{dz^2} - k^2\right) + \omega^2\right] A^S - i\pi\omega\left(A^F - A^S\right) &= 0, \\
\left[c_s^2\left(\frac{d^2}{dz^2} - k^2\right) + \omega^2 + \frac{i\pi\omega^2}{\omega + i\frac{\pi}{r}}\right] B^S &= 0, \\
\left[c_f^{+2}\left(\frac{d^2}{dz^2} - k^2\right) + \omega^2\right] A^{F+} &= 0.
\end{aligned}
\tag{13}
$$

The coefficients A^F, A^S, B^S and A^{F+} are for homogeneous materials independent of z. This leads, in contrast to heterogeneous media where they depend on z, to a differential eigenvalue problem which can be easily solved. Consequently, we seek solutions in the form

$$
\begin{aligned}
A^F &= A_f^1 e^{\gamma_1 z} + A_f^2 e^{\gamma_2 z}, \quad A^S = A_s^1 e^{\gamma_1 z} + A_s^2 e^{\gamma_2 z}, \\
B^S &= B_s e^{\zeta z}, \quad A^{F+} = A_f^+ e^{\gamma^+ z}.
\end{aligned}
\tag{14}
$$

In these relations the exponents $\gamma_1, \gamma_2, \zeta$ must possess negative real parts and γ^+ must possess a positive real part to describe a surface wave. These properties result from Sommerfeld conditions in infinity ($z \to \infty$).

Substitution in (13) yields relations for the exponents: $\frac{\zeta_{1,2}}{k}$ follow from

$$
\left(\frac{\zeta}{k}\right)^2 = 1 - \frac{1}{c_s^2}\left(1 + \frac{i\pi}{\omega + i\frac{\pi}{r}}\right)\left(\frac{\omega}{k}\right)^2,
\tag{15}
$$

$\frac{\gamma_{1,2,3,4}}{k}$ result as solutions of the relation

$$c_f^2\left[\left(\frac{\gamma}{k}\right)^2-1\right]^2+\left[1+\left(1+\frac{1}{r}\right)\frac{i\pi}{\omega}\right]\left(\frac{\omega}{k}\right)^4+ \\ +\left[1+c_f^2+\left(c_f^2+\frac{1}{r}\right)\frac{i\pi}{\omega}\right]\left[\left(\frac{\gamma}{k}\right)^2-1\right]\left(\frac{\omega}{k}\right)^2=0, \tag{16}$$

and $\frac{\gamma_{1,2}^+}{k}$ as solutions of

$$\left(\frac{\gamma^+}{k}\right)^2=1-\frac{1}{c_f^{+2}}\left(\frac{\omega}{k}\right)^2. \tag{17}$$

Simultaneously, we obtain relations for the eigenvectors

$$\mathbf{R}^1=\left(B_s,A_s^1,A_f^1,A^+\right)^T,\quad \mathbf{R}^2=\left(B_s,A_s^2,A_f^2,A^+\right)^T, \tag{18}$$

where

$$A_f^1=\delta_f A_s^1,\quad A_s^2=\delta_s A_f^2, \tag{19}$$

with

$$\delta_f:=\frac{1}{r}\frac{\frac{i\pi}{\omega}\frac{\omega^2}{k^2}}{c_f^2\left[\left(\frac{\gamma_1}{k}\right)^2-1\right]+\left(\frac{\omega}{k}\right)^2+\frac{i\pi}{\omega r}\frac{\omega^2}{k^2}},\qquad \delta_s:=\frac{\frac{i\pi}{\omega}\frac{\omega^2}{k^2}}{\left(\frac{\gamma_2}{k}\right)^2-1+\left(\frac{\omega}{k}\right)^2+\frac{i\pi}{\omega}\frac{\omega^2}{k^2}}. \tag{20}$$

However, we still have four unknown constants B_s, A_f^2, A_s^1, A_f^+ which have to be determined by the boundary conditions.

Complex values of $\zeta_{1,2}$, $\gamma_{1,2,3,4}$ and $\gamma_{1,2}^+$ result from the dissipation caused by the relative motion, i.e. the influence of the permeability π. As a consequence, solutions decay in z-direction but, simultaneously, they vibrate.

3.5 Insertion into boundary conditions

Using the constitutive relations

$$p^F=p_0^F+\kappa\left(\rho^F-\rho_0^F\right),\quad p^{F+}=p_0^{F+}+\kappa^+\left(\rho^{F+}-\rho_0^{F+}\right), \tag{21}$$

and assuming that

$$p_0^{F+}=\frac{p_0^F}{n_0}, \tag{22}$$

which means that the initial external pressure is equal to the initial pore pressure, we insert (8)-(11) into the boundary conditions (5) and obtain in dimensionless form (again omitting the primes)

$$
\begin{aligned}
&\bullet \quad \left(-k^2 B^S - \frac{d^2 B^S}{dz^2} + 2ik\frac{dA^S}{\partial z}\right)\Big|_{z=0} = 0, \\
&\bullet \quad -k^2 A^S + \frac{d^2 A^S}{dz^2} + 2c_s^2\left(k^2 A^S + ik\frac{dB^S}{dz}\right) + \\
&\qquad\qquad + c_f^2 r\left(\frac{d^2 A^F}{dz^2} - k^2 A^F\right) - c_f^{+2} r^+\left(\frac{d^2 A^{F+}}{dz^2} - k^2 A^{F+}\right)\Big|_{z=0} = 0, \\
&\bullet \quad r\left(\frac{dA^F}{\partial z} + ikB^F - \frac{dA^S}{\partial z} - ikB^S\right)\Big|_{z=0} = r^+\left(\frac{dA^{F+}}{\partial z} - \frac{dA^S}{\partial z} - ikB^S\right)\Big|_{z=0}, \\
&\bullet \quad -i\omega\left(\frac{dA^F}{\partial z} + ikB^F - \frac{dA^S}{\partial z} - ikB^S\right)\Big|_{z=0} = \alpha\left\{c_f^2\left(\frac{d^2 A^F}{dz^2} - k^2 A^F\right) - \right. \\
&\qquad\qquad \left. - \underbrace{n_0\frac{r^+}{r}}_{=1} c_f^{+2}\left(\frac{d^2 A^{F+}}{dz^2} - k^2 A^{F+}\right)\right\},
\end{aligned}
\tag{23}
$$

where we have used the relation $n_0 = \frac{r}{r^+}$ if $r^+ \neq 0$.

3.6 Dispersion relation

Inserting the ansatz for the solutions (14) into these boundary conditions we obtain the following problem for the four unknown constants B_s, A_s^1, A_f^2, A_f^+

$$
\mathbf{AX} = \mathbf{0}, \tag{24}
$$

where

$$
\mathbf{A} := \begin{pmatrix}
\left(\frac{\zeta}{k}\right)^2 + 1 & -2i\frac{\gamma_1}{k} \\
2ic_s^2\frac{\zeta}{k} & \left(\frac{\gamma_1}{k}\right)^2 - 1 + 2c_s^2 + \\
& + rc_f^2\left[\left(\frac{\gamma_1}{k}\right)^2 - 1\right]\delta_f \\
-\frac{\pi}{r\omega + i\pi} + i\left(\frac{r^+}{r} - 1\right) & \frac{\gamma_1}{k}\left[\delta_f + \left(\frac{r^+}{r} - 1\right)\right] \\
\frac{r\omega}{r\omega + i\pi}\frac{\omega}{k} & i\frac{\omega}{k}\frac{\gamma_1}{k}(\delta_f - 1) + \\
& + \alpha c_f^2\left[\left(\frac{\gamma_1}{k}\right)^2 - 1\right]\delta_f
\end{pmatrix}
\tag{25}
$$

$$
\begin{pmatrix}
-2i\frac{\gamma_2}{k}\delta_s & 0 \\
\left[\left(\frac{\gamma_2}{k}\right)^2 - 1 + 2c_s^2\right]\delta_s + & -r^+ c_f^{+2}\left[\left(\frac{\gamma^+}{k}\right)^2 - 1\right] \\
+rc_f^2\left[\left(\frac{\gamma_2}{k}\right)^2 - 1\right] & \\
\frac{\gamma_2}{k}\left[1 + \delta_s\left(\frac{r^+}{r} - 1\right)\right] & -\frac{r^+}{r}\frac{\gamma^+}{k} \\
i\frac{\omega}{k}\frac{\gamma_2}{k}(1-\delta_s) + & \\
+\alpha c_f^2\left[\left(\frac{\gamma_2}{k}\right)^2 - 1\right] & -\alpha c_f^{+2}\left[\left(\frac{\gamma_+}{k}\right)^2 - 1\right]
\end{pmatrix}, \qquad (25)_{\text{cont.}}
$$

$$
\mathbf{X} := \left(\; B_s, \quad A_s^1, \quad A_f^2, \quad A_f^+ \; \right)^T. \qquad (26)
$$

This homogeneous set yields the *dispersion relation:* $\det \mathbf{A} = 0$ determining the $\omega - k$ relation.

3.7 High and low frequency approximations

High frequencies In the case of high frequencies (physical dimensions) $\frac{1}{\omega\tau} \ll 1$ we have $\delta_s = \delta_f = 0$ and the exponents $\left(\frac{\gamma_1}{k}\right)^2 = 1 - \left(\frac{\omega}{k}\right)^2$, $\left(\frac{\gamma_2}{k}\right)^2 = 1 - \frac{1}{c_f^2}\left(\frac{\omega}{k}\right)^2$, $\left(\frac{\zeta}{k}\right)^2 = 1 - \frac{1}{c_s^2}\left(\frac{\omega}{k}\right)^2$ and $\left(\frac{\gamma^+}{k}\right)^2 = 1 - \frac{1}{c_f^{+2}}\left(\frac{\omega}{k}\right)^2$. The dispersion relation follows in the form

$$
\begin{aligned}
\alpha\frac{r}{c_s^4}\frac{r}{r^+}\left(\frac{r^+}{r} - 1\right)^2\frac{\gamma_1}{k}\left(\frac{\omega}{k}\right)^5 + i\frac{r}{c_s^4}\left(\frac{\gamma^+}{k} - \frac{r^+}{r}\frac{\gamma_2}{k}\right)\frac{\gamma_1}{k}\left(\frac{\omega}{k}\right)^4 + \\
+\alpha\mathcal{P}_R\left(\frac{r}{r^+}\frac{\gamma_2}{k} - \frac{\gamma^+}{k}\right)\frac{\omega}{k} + i\frac{\gamma_2}{k}\frac{\gamma_+}{k}\mathcal{P}_R = 0,
\end{aligned} \qquad (27)
$$

where

$$
\mathcal{P}_R := \left[2 - \frac{1}{c_s^2}\left(\frac{\omega}{k}\right)^2\right]^2 - 4\frac{\gamma_1}{k}\frac{\zeta}{k}. \qquad (28)
$$

This is the classical Rayleigh dispersion relation. We consider two cases of the dispersion relation (27):

1. $\underline{\alpha = 0}$ (impermeable boundary; i.e. sealed porous medium in contact with an external fluid)

   We get from (27)
   $$
   \frac{\gamma_+}{k}\frac{\gamma_2}{k}\mathcal{P}_R + \left(\frac{\gamma^+}{k} - \frac{r^+}{r}\frac{\gamma_2}{k}\right)\frac{r}{c_s^4}\frac{\gamma_1}{k}\left(\frac{\omega}{k}\right)^4 = 0. \qquad (29)
   $$

   The case $\alpha = 0$ does not correspond to the case of the boundary porous medium/vacuum because the fluid outside of the porous medium yields a pressure on the boundary. However, if additionally to $\alpha = 0$ also $r^+ = 0$ we have the same conditions

and (29) must be identical to the Rayleigh dispersion relation for the boundary porous medium/vacuum (see e.g.: [24])

$$\mathcal{P}_V = \mathcal{P}_R \frac{\gamma_2}{k} + \frac{r}{c_s^4} \frac{\gamma_1}{k} \left(\frac{\omega}{k}\right)^4 = 0. \tag{30}$$

This is, indeed, true if we cancel $\frac{\gamma^+}{k}$ on both sides after setting r^+ equal to zero.

2. $\underline{\alpha \to \infty}$
Here, the other two terms of (27) remain and we obtain after division by α

$$\mathcal{P}_R \left(\frac{\gamma_2}{k} - \frac{r^+}{r}\frac{\gamma^+}{k}\right) + \left(\frac{r^+}{r} - 1\right)^2 \frac{r}{c_s^4} \frac{\gamma_1}{k} \left(\frac{\omega}{k}\right)^4 = 0. \tag{31}$$

Both equations (29) and (31) remind equation (30) but they are both modified by the influence of the fluid outside.

Low frequencies In contrast to the impermeable boundary with vacuum analytical calculations in this case become very complicated. Therefore, we investigate this case solely on a numerical example.

4 Numerical results

4.1 Procedure and parameters

The problem $\det \mathbf{A} = 0$ has been solved for the complex wave number, k, using the two computing packages MAPLE 7 and MAPLE V Release 5.1. In principle, it is possible to use the existing equation solvers although, for the calculations with complex variables, one has to perform a very careful manual bookkeeping and, in addition, they need a very extensive main memory. This makes the numerical evaluation far from being trivial. It has been observed that the used packages calculate only *one of the solutions* for k for any choice of sign combinations of exponents $\gamma_1, \gamma_2, \gamma^+$ and ζ, changing between branches of solution by the variation of exponents without any apparent reason. Interestingly, the programs for some sign combination of exponents produce two solutions which are close to each other but, for most frequencies, not the same.

Inspection of the above solutions shows that they contain roots of quantities which are either already complex or may change the sign. As well known, this means that there exist many Riemann surfaces. It has been seen already in the case of classical Rayleigh waves ([16], [19]) that, in order to obtain a true surface wave one has to choose a proper Riemann plane otherwise one obtains leaky surface waves. This is, of course, also visible in the numerical procedure which yields solutions on both Riemann surfaces which are related to the true surface wave as well as to solutions for leaky waves. An additional problem arises due to the fact that complex solutions in the present case follow not only from the choice of the Riemann surface but also from the attenuation through dissipation. Consequently, a numerical analysis has to be done with a particular care.

From the complex results for k we are able to determine the normalized velocities of the surface waves $c' = \frac{\omega}{\mathrm{Re}\, k_i}$, and the corresponding normalized attenuations $\mathrm{Im}\, k_i$.

The calculations have been performed for the following data which correspond to water saturated sandstones:

$$
\begin{aligned}
&c_{P1} = 2500\ \frac{\mathrm{m}}{\mathrm{s}}, \quad && c_{P2} = 1000\ \frac{\mathrm{m}}{\mathrm{s}}, \quad && c_S = 1250\ \frac{\mathrm{m}}{\mathrm{s}}, \quad && c_+ = 1500\ \frac{\mathrm{m}}{\mathrm{s}},\\
&\rho_0^S = 2500\ \frac{\mathrm{kg}}{\mathrm{m}^3}, \quad && \rho_0^F = 250\ \frac{\mathrm{kg}}{\mathrm{m}^3}, \quad && \rho_0^{F+} = 1000\ \frac{\mathrm{kg}}{\mathrm{m}^3}, \quad && r = \frac{\rho_0^F}{\rho_0^S} = 0.1,\\
&c_f = \frac{c_{P2}}{c_{P1}} = 0.4, \quad && c_s = \frac{c_S}{c_{P1}} = 0.5, \quad && c_f^+ = \frac{c_+}{c_{P1}} = 0.6, \quad && r^+ = \frac{\rho_0^{F+}}{\rho_0^S} = 0.4.
\end{aligned}
\tag{32}
$$

While some of the results for the boundary porous medium/vacuum have been shown for the varying bulk permeability parameter, π, this coefficient is constant here, namely $\pi = 10^7\ \frac{\mathrm{kg}}{\mathrm{m}^3\mathrm{s}}$. [b] However, instead of this we show for this boundary the influence of the surface permeability, α. We demonstrate that two surface waves, both of them leaky, exist in the whole range of frequencies for each choice of α. They correspond to the classical Rayleigh wave, and to a Stoneley wave which is produced due to presence of the fluid outside the porous medium, respectively. The latter can be supported by the fact that it appears also for the sealed pore situation if there is a fluid outside. Moreover we obtain a third type of wave which appeared also on the boundary porous medium/vacuum, namely a true Stoneley wave. However, this wave exists only for small values of α.

Numerical results for velocities are normalized by the $P1$-velocity. Imaginary parts of the wave number k determine the damping of waves. It is normalized by the product with the $P1$-velocity and the relaxation time (see: (12)). This means for our parameters that the values presented in the figures are 400 times smaller ($(2500 \times 10^{-6})^{-1}$) than in real physical units $\left[\frac{1}{\mathrm{m}}\right]$.

4.2 Dependence of phase velocities and attenuations on the frequency

To have an impression of the results of the simpler problem of the boundary between a porous medium and a vacuum and in order to compare them to the results on the present problem Fig. 3 is included. It shows the normalized velocities and attenuations of both the leaky Rayleigh wave and the true Stoneley wave which appear at this boundary.

Fig. 5 shows both the phase velocities and the attenuations of all three surface waves appearing at the interface between a porous halfspace and a fluid halfspace. On the left hand side the velocities are plotted and figures on the right hand side show the attenuations. Both quantities are given for a wide range of frequencies between 1 Hz and 100 MHz. The different curves correspond to various values of the surface permeability parameter α. As explained above, $\alpha = 0$ means that the surface is completely impermeable while $\alpha = \infty$ corresponds to an open pore situation.

Both the frequency and the attenuations are shown in logarithmic scale while the velocity

[b] For instance, for water saturated sands $K \sim 10^{-2} \div 10^{-3}\ \frac{\mathrm{m}}{\mathrm{s}}$, $\rho \sim 10^3\ \frac{\mathrm{kg}}{\mathrm{m}^3}$ and $g \sim 10\ \frac{\mathrm{m}}{\mathrm{s}^2} \Longrightarrow \pi \sim 10^6 \div 10^7\ \frac{\mathrm{kg}}{\mathrm{m}^3\mathrm{s}}$ (see e.g. Bear [5]). In standard units of permeability this corresponds to app. $1 \div 0.1$ darcy.

is presented in normal scale.

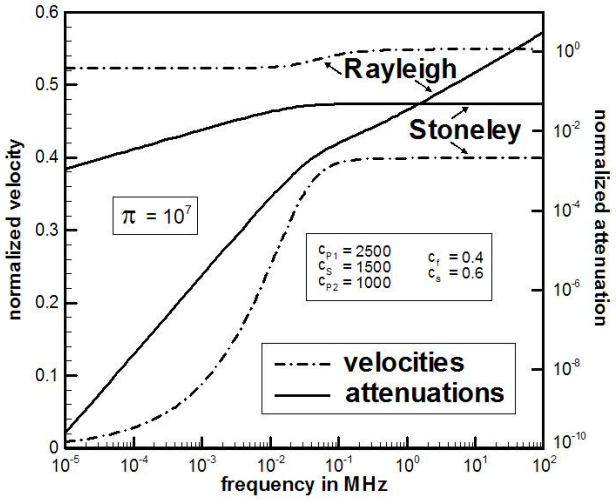

Fig. 3: Normalized phase velocities and attenuations of the leaky Rayleigh and the true Stoneley wave appearing on the boundary between a poroelastic medium and vacuum in dependence on the frequency.

4.2.1 Phase velocities

The velocity of the Rayleigh wave lies under the velocity of the bulk shear wave, c_S, whose normalized value is $c_s \equiv \frac{c_S}{c_{P1}} = 0.5$. Curves for different values of α have each a low and a high frequency limit which is unequal to zero. While for small frequencies the velocity is the same independently of α, the high frequency limit decreases with increasing α. For the open pore situation the difference between high and low frequency limits is approximately one half of the difference for a close boundary. Inbetween there is a steep increase of the Rayleigh velocity. The range of frequencies for this increase is smaller for small values of α (10-100 kHz) than for large values of α (1-500 kHz). Moreover, for the latter, there appears a small plateau in this zone. This may be an indication of the change of the Riemann surface which is, however, much better pronounced in the attenuations.

The velocity of the leaky Stoneley wave behaves similar to the Rayleigh wave. Also this wave possesses high an low frequency limits unequal to zero and the steep increase inbetween appears in the same frequency region. However, in contrast to the Rayleigh wave for this wave the high frequency limit is larger for bigger values of α than for smaller ones. The frequency behavior of this wave is – at least for small α – not monotonous. A maximum value appears in the region of order 100 kHz. Interestingly, the velocity of this wave is smaller than this of the Rayleigh wave although it is driven by the fluid outside of the porous medium whose longitudinal bulk wave is faster than that of the fluid inside the porous medium ($c_f^+ = 0.6$, $c_f = 0.4$). This result has been obtained also by Feng & Johnson [12] within Biot's model. As we will see in subsection 4.3 the true Stoneley wave exists only for small values of α, and, therefore, we show its behavior only for two values of α. For these the velocities do not differ substantially. They start form zero at $\omega = 0$ and increase until around 100 kHz where they reach a high frequency limit which is a little bit smaller than the velocity of the $P2$ wave, $c_f \equiv \frac{c_{P2}}{c_{P1}} = 0.4$.

4.2.2 Attenuations

Let us start with the attenuation of the true Stoneley wave. This has the same appearance as that obtained for the boundary porous medium/vacuum (see also: Fig. 3). We show a log-log-plot of this attenuation. The attenuation starts from zero as $\omega = 0$ and reaches a horizontal asymptote at around 100 kHz. The only amazing point is, that in the mapped region of frequencies, starting from 1 Hz the value for $\alpha = 10^{-4}\ \frac{\mathrm{s}}{\mathrm{m}}$ is much smaller than for $\alpha = 0$ even though the difference in velocities is small. It is surprising because for the other attenuations the value for $\alpha = 0$ lies under all other values for different α.

In contrast to the true surface wave the remaining leaky waves possess singularities in the attenuation for two intermediate frequencies. These frequencies seem to be related to characteristic frequencies $\frac{\pi}{2\rho_0^S}$ and $\frac{\pi}{2\rho_0^F}$ which have already appeared in the stability analysis of adsorption processes [2]. However, there exists an influence of the parameter α, responsible for dissipation, and, simultaneously, the location of the singularities changes with the variation of this coefficient. Consequently, as indicated also in some papers on Biot's model, the diffusion-driven resonances appear also in the surface waves. Their existence seems to be confirmed experimentally (for results of measurements see in particular [8], [25]). On the right we reproduce one figure of the paper [8]. It shows the measured damping coefficients of the pseudo-Stoneley wave (in our terminology: leaky Stoneley wave) in a shock-induced borehole experiment. The formation is a Berea sandstone. The damping coefficient is given in a frequency range up to 50 kHz and we see that there appear also some well pronounced singularities.

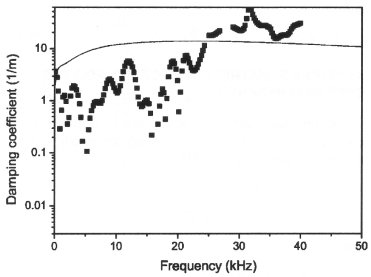

Fig. 4: Experimental damping coefficients of the pseudo-Stoneley wave. (quoted after [8]).

Little is known about their mathematical origin. However, the numerical analysis indicates that they appear due to the change of the Riemann surface. If one would ignore the singularities and look only at the connecting line between the maxima the curves would look similar to the curve for the boundary porous medium/vacuum.

In any case, it is obvious that the curves show the leaky character as observed already for the Rayleigh wave for this boundary: for high frequencies the attenuation grows linearly and unbounded.

4.3 Dependence of phase velocities and attenuations on the surface permeability

In Figure 6 we illustrate the behavior of the three surface waves appearing at the boundary porous medium/fluid for the frequency limits $\omega \to \infty$, $\omega \to 0$ but in dependence on the surface permeability parameter α. In the first row of Fig. 6 we show normalized velocities and attenuations for the same material parameters as used in the last subsection. In the bottom row the same quantities are shown for another choice of material parameters: with unchanged mass densities and porosity and different velocities for two bulk waves ($c_{P1} = 3500\ \frac{\mathrm{m}}{\mathrm{s}}$, $c_S = 1750\ \frac{\mathrm{m}}{\mathrm{s}}$, c_{P2}, c_{P+} unchanged).

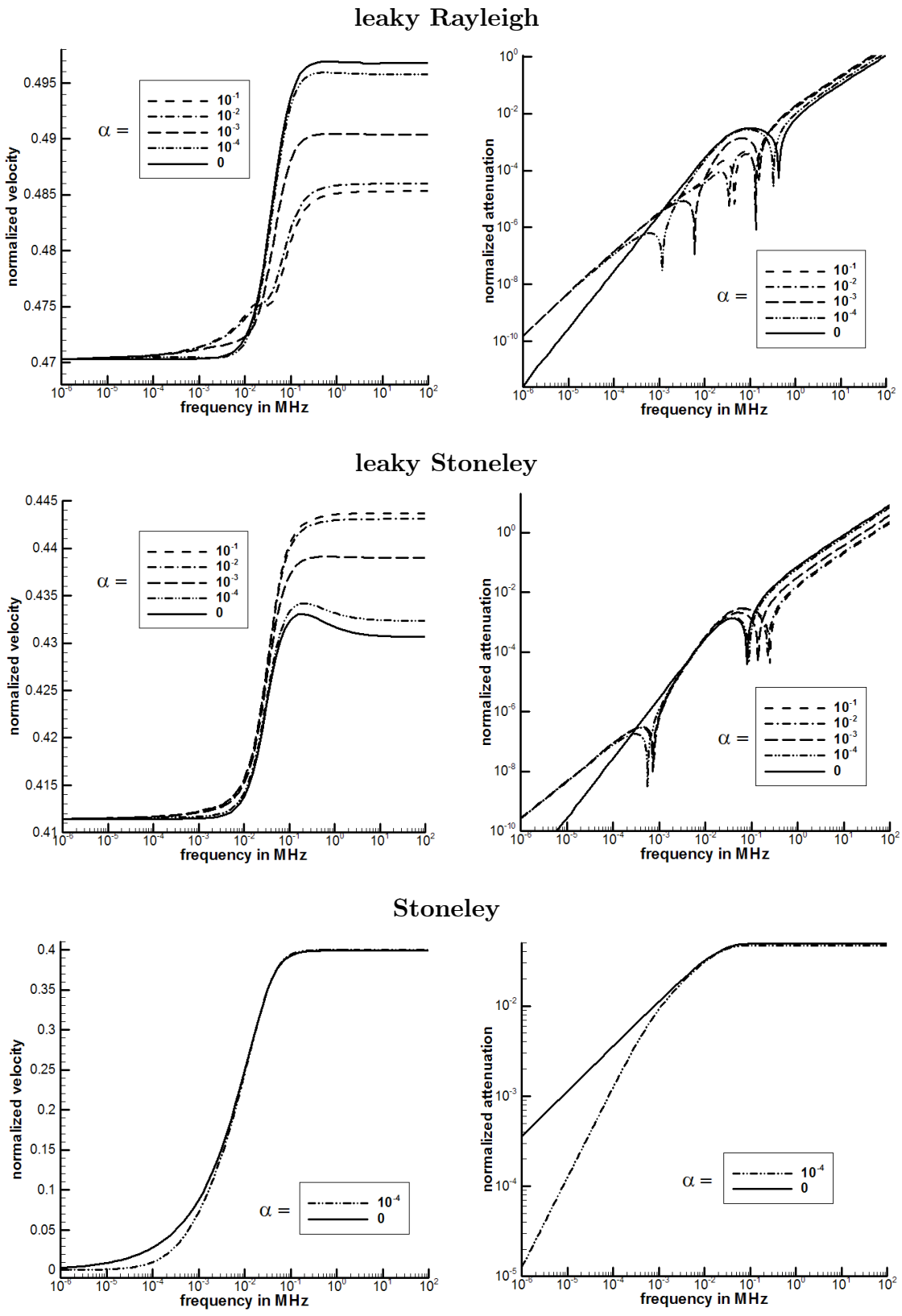

Fig. 5: Normalized phase velocities and attenuations of the leaky Rayleigh, leaky Stoneley and the Stoneley wave in dependence on the frequency. Different curves correspond to different values of the surface permeability α (in units $\left[\frac{\mathrm{s}}{\mathrm{m}}\right]$).
The smaller α the denser the boundary.

The upper left figure shows the phase velocities of the surface waves for the two limits of frequencies ($\omega \to \infty$ – solid lines, $\omega \to 0$ – dashed lines). Additional to the shown range of surface permeability parameters between 10^{-6} $\frac{\mathrm{s}}{\mathrm{m}}$ and 10^{-1} $\frac{\mathrm{s}}{\mathrm{m}}$ we show on the left and right hand side points corresponding to the limit cases $\alpha = 0$ and $\alpha = \infty$. It is obvious that the values for 10^{-6} and 10^{-1} correspond already well to the limit values. While both leaky surface waves exist in the whole range of surface permeabilities, the true surface wave appears only for small values of the surface permeability (approx. in the interval $0 \leq \alpha \leq 10^{-3.9}$ $\frac{\mathrm{s}}{\mathrm{m}}$).
Thus for a relatively open boundary (large α) no real surface wave exists.
It is obvious that for each wave the low frequency value of the velocity (dashed lines) is independent of α. For the true surface wave this value is zero while it is bigger than zero for the leaky waves. Both the high frequency limit of the leaky Rayleigh and of the leaky Stoneley wave change monotonously from the limit $\alpha = 0$ to the limit $\alpha = \infty$. However, the Rayleigh wave velocity is bigger for a dense boundary, while for the leaky Stoneley wave the limit for the open boundary is bigger. The velocity behavior of the waves for the other choice of material parameters ($c_S > c_{f+}$, see: bottom left figure) does not change substantially. Again, $c_R < c_s$, $c_{St} < c_f$ and $c_{leakySt} < c_{f+}$. The latter is a little bit more obvious for this choice of material parameters than for the other choice. As shown above the last choice corresponds to a higher value of the modulus of the skeleton frame (5.53 instead of 3.95). For this stiffer medium the true Stoneley wave exists only for a still denser boundary, namely for approx. $0 \leq \alpha \leq 10^{-4.8}$ $\frac{\mathrm{s}}{\mathrm{m}}$).

The figures on the right hand side show the normalized attenuation of the three surface waves for a chosen frequency. As already mentioned, the true surface wave – the Stoneley wave – ceases to exist in the range of high surface permeabilities α. In the limit value, its attenuation becomes infinite. The remaining two leaky waves possess finite attenuation in the whole range of α.

4.4 Group velocities of the three surface waves

The figures for phase velocities of Rayleigh and Stoneley waves show that both of them depend on the frequency ω. In inhomogeneous media waves of different frequency (or wavelength) in general propagate with different phase velocities. This phenomenon is known as *dispersion*. The dispersion in heterogeneous materials appears in a nondissipative manner which is not the case in systems with diffusion. It is easy to see that dissipative waves considered in this article become nondispersive in the nondissipative limit $\pi \to 0$.

A monochromatic wave as investigated in this section is an idealization which is never strictly realized in nature. Most sources emit signals with a continuous spectrum over a limited frequency band. The group velocity c_g (for details in the case of real k see e.g. [1], [6] or [26]) for a given frequency ω is the velocity of transport of a wave package consisting of contributions from a band of frequencies around ω. Then, accounting for the fact that the real wavelength k and the phase velocity c_{ph} depend on the frequency $\left(k = \frac{\omega}{c_{ph}}\right)$

$$\frac{dk}{d\omega} = \frac{1}{c_g} = \frac{1}{c_{ph}} - \frac{\omega}{c_{ph}^2}\frac{dc_{ph}}{d\omega}, \quad \Rightarrow c_g = \frac{c_{ph}}{1 - \frac{\omega}{c_{ph}}\frac{dc_{ph}}{d\omega}}. \tag{33}$$

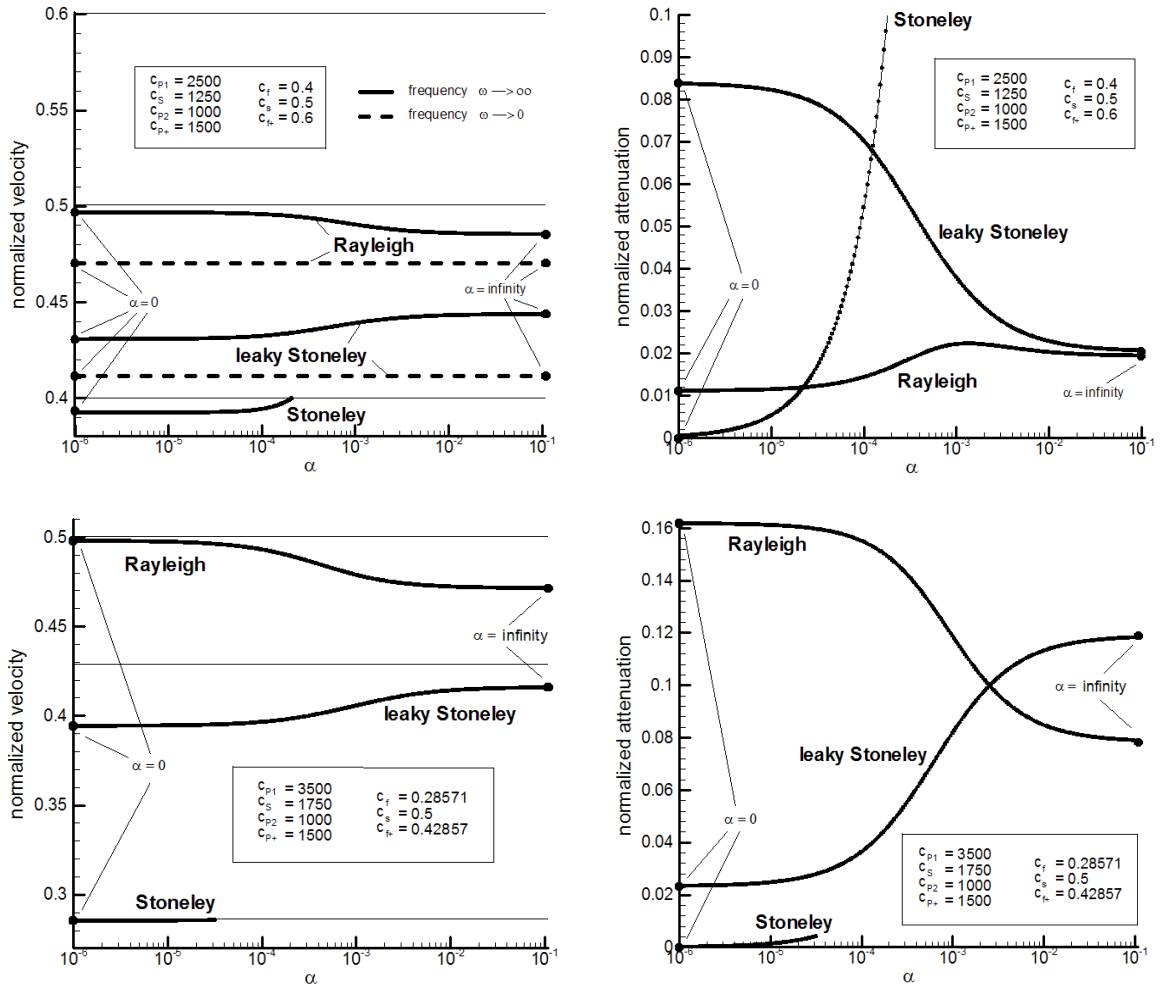

Fig. 6: Normalized phase velocities and attenuations of the three surface waves in dependence on the surface permeability parameter, α, for different material parameters.

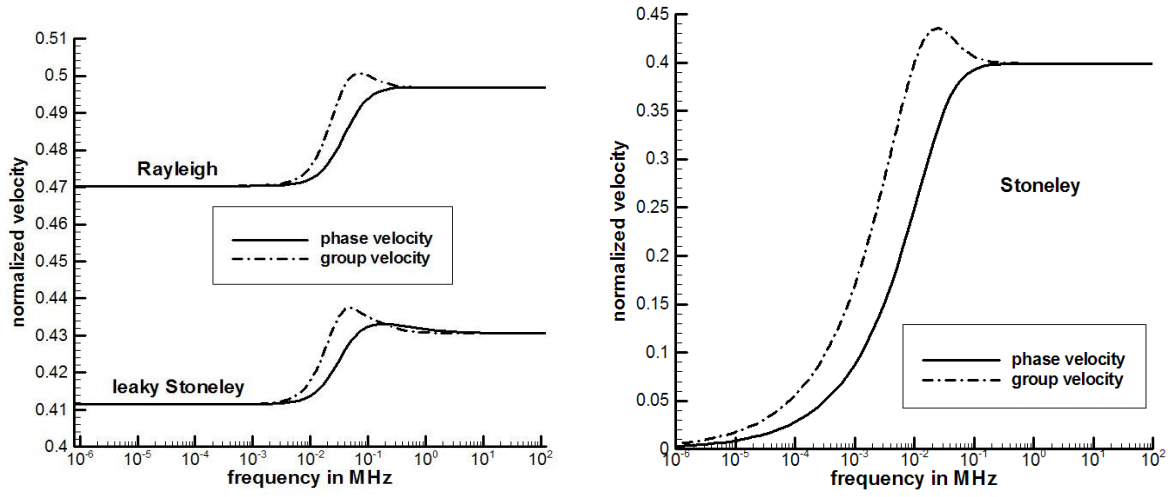

Fig. 7: Normalized phase and group velocities of the three surface waves.

However, in our case the wave number is complex ($k = k_R(\omega) + ik_I(\omega)$) and a relation similar to (33) follows under some simplifying assumptions. We consider the wave consisting of a narrow band of frequencies near the middle frequency ω_0. The solution for the amplitude A can be described by a Fourier integral which accounts for all frequencies entering the band

$$A(x,t) = \frac{1}{2\pi}\int_{-\infty}^{\infty} A(\omega)\, \mathrm{e}^{-k_I x}\, \mathrm{e}^{i(k_R x - \omega t)}\, d\omega. \tag{34}$$

Under the assumptions of small changes of the amplitude and small changes of damping k_I in the range $\omega_0 \le \omega \le \omega_0 + \Delta\omega$, this is approximately

$$\begin{aligned}
A(x,t) &\cong \frac{1}{2\pi} A(\omega_0)\, \mathrm{e}^{-k_I^0 x}\, \mathrm{e}^{i\left(k_R^0 x - \omega_0 t\right)} \int_{\omega_0}^{\omega_0+\Delta\omega} \mathrm{e}^{i\left(\frac{x}{c_g} - t\right)(\omega-\omega_0)}\, d\omega \cong \\
&\cong \frac{1}{2\pi} A(\omega_0)\, \mathrm{e}^{i(k_0 x - \omega_0 t)} \int_0^{\Delta\omega} \mathrm{e}^{i\left(\frac{x}{c_g} - t\right)\xi}\, d\xi = \\
&= \frac{1}{2\pi} A(\omega_0)\, \mathrm{e}^{i(k_0 x - \omega_0 t)} \int_0^{\Delta\omega} \left[\cos\left(\frac{x}{c_g} - t\right)\xi + i \sin\left(\frac{x}{c_g} - t\right)\xi\right] d\xi = \\
&= \frac{1}{2\pi} A(\omega_0)\, \mathrm{e}^{i(k_0 x - \omega_0 t)}\, \frac{1}{\frac{x}{c_g} - t} \left[\sin\left(\frac{x}{c_g} - t\right)\Delta\omega - i \underbrace{\left(\cos\left(\frac{x}{c_g} - t\right)\Delta\omega - 1\right)}_{\approx 0}\right] = \\
&= \frac{1}{2\pi} A(\omega_0) \underbrace{\mathrm{e}^{ik_0\left(x - c_{ph} t\right)}}_{\text{carrier}} \underbrace{\left(\frac{\sin\left[\left(\frac{x}{c_g} - t\right)\Delta\omega\right]}{\left(\frac{x}{c_g} - t\right)\Delta\omega}\right)}_{\text{modulator}} \Delta\omega,
\end{aligned} \tag{35}$$

with $\boxed{c_g := \left(\frac{dk_R}{d\omega}\right)^{-1}_{\omega=\omega_0} = \frac{c_{ph}}{1 - \frac{\omega}{c_{ph}}\frac{dc_{ph}}{d\omega}}}$ and $\left|\frac{\Delta\omega}{\omega_0}\right| \ll 1, \quad c_{ph} = \frac{\omega}{k_R}$

$$k_0 = k_R^0 + ik_I^0 = k(\omega_0).$$

For the impermeable boundary ($\alpha = 0$) between a porous material and a fluid we present in Fig. 7 the group velocities of the surface waves. The group velocity of the leaky Stoneley wave behaves differently from the both waves which also appeared for the boundary porous medium/vacuum. While they only possess a maximum for a certain frequency, the leaky Stoneley wave exhibits first a strong minimum and then a slight maximum. The mathematical reason is obvious: the growth in phase velocities of Rayleigh and Stoneley waves is almost monotonous but for the leaky Stoneley wave the phase velocity possesses a clear maximum (compare: Fig. 5), and, as indicated in the box of (35) the group velocity depends on the slope of the phase velocity.
It is clearly seen that the maximum group velocities exceed the corresponding limit values of the bulk waves. This indicates that surface waves cannot exist in the vicinity of the maximum point. Consequently, if we account for the resonance behavior indicated in Fig. 5, the range of frequencies between two resonances is most likely forbidden for the propagation of surface waves.

5 Summary of results and conclusions

In the whole range of frequencies there exist two leaky surface waves: a leaky Rayleigh wave and a leaky Stoneley wave. In the range of very small values of the surface permeability parameter α, there exists a third true surface wave – a Stoneley wave. They possess the following attributes:

Leaky Rayleigh

- the velocity of propagation of this wave lies in the interval determined by the limits $\omega \to 0$ and $\omega \to \infty$. The high frequency limit is higher than the low frequency limit. The velocity is always smaller than c_S, i.e. slower than the S-wave. As a function of ω it possesses at least one inflection point.

- for low frequencies the phase velocity for different values of the surface permeability α remains almost constant. For high frequencies smaller values of α yield bigger velocities; for the open pore case the difference between high and low frequency limits is approx. one half of the difference for a close boundary;

- the attenuation grows linearly and unbounded (the feature of a leaky wave), there appear singularities which depend on α and seem to be related to the characteristic frequencies $\frac{\pi}{2\rho_0^S}$ and $\frac{\pi}{2\rho_0^F}$;

Leaky Stoneley

- the phase velocity of this wave behaves similarly to this of the leaky Rayleigh wave; however, the high frequency limit is larger for bigger values of α than for smaller ones; a maximum value appears in the region of order 100 kHz; the velocity of the leaky Stoneley wave is for each pair (ω, α) smaller than this of the leaky Rayleigh wave.

- also the attenuation behaves similar to this of the leaky Rayleigh wave; however, the singularities are weaker dependent on α;

True Stoneley

- it exists only for small values of the surface permeability α; for different values of α the velocity is nearly the same; it grows monotonically from the zero value for $\omega = 0$ to a finite limit which is slightly smaller (approx. 0.15%) than the velocity c_{P2} of the $P2$-wave. The growth of the velocity of this wave in the range of low frequencies is much steeper than this of Rayleigh waves similarly to the growth of the $P2$-velocity;

- both the velocity and attenuation of the true Stoneley wave approach zero as $\sqrt{\omega}$ (which is not directly obvious due to the logarithmic scale of the figures);

- the attenuation of the Stoneley wave grows monotonically to a finite limit for $\omega \to \infty$. It is slightly smaller than the attenuation of $P2$-waves.

The above described results show that the behavior of true and leaky surface waves at intermediate frequencies s far from being trivial and cannot be ignored. Simultaneously, a rather sophisticated numerical analysis which yields this conclusion demonstrates that, at least at the present stage of evolution of numerical methods, the analysis of the full Biot model is technically almost impossible.
Let us add that neither finite element calculations nor boundary element calculations can be applied to this analysis. The first one is not appropriate in the case of infinite problems (Sommerfeld conditions) and the second one requires the knowledge of the dynamical GREENs function which is known only for some simplified problems ($\pi \approx 0$ – no diffusion, and, consequently, no attenuation due to dissipation).

References

[1] K. Aki, P. Richards: *Quantitative seismology, theory and methods,* W. H. Freeman and Co. (1980).

[2] B. Albers: Relaxation Analysis and Linear Stability vs. Adsorption in Porous Materials, *Continuum Mech. Thermodyn.*, **15** (2003) 1, 73-95, also WIAS-Preprint Nr. 721, 2002.

[3] B. Albers, K. Wilmanski: On modeling acoustic waves in saturated poroelastic media, *ASCE-J.Engn.Mech.*, **131**, 5 (2005), also WIAS-Preprint No. 874 (2003).

[4] B. Albers, K. Wilmanski: Monochromatic surface waves on impermeable boundaries in two-component poroelastic media, submitted to *Continuum Mech. Thermodyn.*, also WIAS-Preprint No. 862 (2003).

[5] J. Bear, *Dynamics of Fluids in Porous Media,* Dover Publications, New York (1988).

[6] A. Ben-Menahem, S. J. Singh: *Seismic waves and sources*, Dover (1981).

[7] M. A. Biot: *Acoustics, elasticity and thermodynamics of porous media: Twenty-one papers by M. A. Biot*, edited by I. Tolstoy, American Institute of Physics (1992).

[8] G. Chao, D. M. J. Smeulders, M. E. H. van Dongen: Shock induced borehole waves in porous formations: Theory and experiments, *J. Acoust. Soc. Am.* **116 (**2), 693-702, (2004).

[9] H. Deresiewicz: The effect of boundaries on wave propagation in a liquid filled porous solid. IV. Surface waves in a half space, *Bull. Seismol. Soc. Am.*, **52**, 627-638 (1962).

[10] H. Deresiewicz, R. Skalak: On uniqueness in dynamic poroelasticity, *Bull. Seismol. Soc. Am.*, **53**, 783-788 (1963).

[11] I. Edelman, K. Wilmanski: Asymptotic analysis of surface waves at vacuum/porous medium and liquid/porous medium interfaces, *Cont. Mech. Thermodyn.*, 25-44, **14**, 1 (2002).

[12] S. Feng, D. L. Johnson: High-frequency acoustic properties of a fluid/porous solid interface. I. New surface mode, *J. Acoust. Soc. Am.*, **74**(3), 906-914 (1983), II. The 2D reflection Green's function, *J. Acoust. Soc. Am.*, **74**(3), 915-924 (1983).

[13] A. A. Gubaidullin, O. Y. Kuchugurina, D. M. J. Smeulders, C. J. Wisse: Frequency-dependent acoustic properties of a fluid/porous solid interface, *J. Acoust. Soc. Am.*, **116**(3), 1474-1480 (2004).

[14] R. A. Phinney: Propagation of leaking interface waves, *Bull. Seismol. Soc. Am.*, **51**(4), 527-555 (1961).

[15] G. J. Rix, C. G. Lai, S. Foti: Simultaneous measurement of surface wave dispersion and attenuation curves, *Geotechnical Testing Journal*, 24(4), 350-358 (2001).

[16] C. T. Schröder, W. R. Scott Jr.: On the complex conjugate roots of the Rayleigh equation: The leaky surface wave, *J. Acoust. Soc. Am.,* **110** (6), 2867-2877 (2001).

[17] A. Udias: *Principles of Seismology*, Cambridge University Press (1999).

[18] I. A. Viktorov, *Rayleigh and Lamb waves. physical theory and applications,* Plenum Press, New York (1967).

[19] K. Wilmanski: Elastic modelling of surface waves in single and multicomponent systems, in: *Surface Waves in Geomechanics, Direct and Inverse Modelling for Soils and Rocks*, C. Lai, K. Wilmanski (eds.), CISM Courses and Lectures, Springer Wien New York (2005).

[20] K. Wilmanski: Tortuosity and objective relative acceleration in the theory of porous materials, *Proc. Royal Soc. London, A,* vol. 461 #2056 (2005), also WIAS-Preprint No. 922 (2004).

[21] K. Wilmanski: Propagation of sound and surface waves in porous materials, in: *Structured media* edited by B. Maruszewski, Poznan University of Technology, Poznan (2002), pp. 312-326.

[22] K. Wilmanski: Some questions on material objectivity arising in models of porous materials, in *Rational continua, classical and new,* edited by M. Brocato, Springer-Verlag, Italia Srl, Milano (2001), pp.149-161.

[23] K. Wilmanski: Waves in porous and granular materials, in: *Kinetic and continuum theories of granular and porous media*, edited by K. Hutter and K. Wilmanski, CISM Courses and Lectures No. 400, Springer Wien New York (1999), pp. 131-186.

[24] K. Wilmanski, B. Albers: Acoustic waves in porous solid-fluid mixtures, in: *Dynamic response of granular and porous materials under large and catastrophic deformations*, edited by K. Hutter and N. Kirchner, Lecture Notes in Applied and Computational Mechanics, Vol.11, Springer, Berlin (2003), pp. 285-314.

[25] C. J. Wisse, D. M. J. Smeulders, M. E. H. van Dongen, G. Chao: Guided wave modes in porous cylinders: Experimental results, *J. Acoust. Soc. Am.*, **112**(3), 890-895 (2002).

[26] G. B. Whitham: *Linear and nonlinear waves*, John Wiley & Sons, New York (1974).